Cyanide-modified Pt(1 1 1): Structure, stability and hydrogen adsorption

María Escudero-Escribano [a], Germán J. Soldano [b], Paola Quaino [b,c], Martín E. Zoloff Michoff [d], Ezequiel P.M. Leiva [d], Wolfgang Schmickler [b], Ángel Cuesta [a,*]

[a] Instituto de Química Física "Rocasolano", CSIC, C. Serrano 119, E-28006 Madrid, Spain
[b] Institut für Theoretische Chemie, Universitat Ulm, D-89069 Ulm, Germany
[c] PRELINE, Facultad de Ingeniería Química, Universidad Nacional del Litoral, 3000 Santa Fe, Argentina
[d] INFIQC, Departamento de Matemática y Física, Facultad de Ciencias Químicas, Universidad Nacional de Córdoba, Córdoba, Argentina

A R T I C L E   I N F O

A B S T R A C T

Cyanide-modified Pt(1 1 1) surfaces have been recently used to study atomic-ensemble effects in electrocatalysis. These studies have been based on the assumption that cyanide acts as a third body, blocking some surface sites but leaving the electronic properties of the surrounding ones unaltered, although this is in apparent contradiction with the observation of a positive shift of 0.2 V in the onset of hydrogen adsorption on cyanide-modified Pt(1 1 1) electrodes, as compared with clean Pt(1 1 1). We have performed theoretical calculations in order to provide support to this assumption and explain the positive shift in the onset of hydrogen adsorption, which is shown to be due to the formation of CNH_{ad}.

1. Introduction

The adsorption of cyanide on single-crystal platinum electrodes has been intensively investigated over the last two decades, partly because cyanide and carbon monoxide are isoelectronic [1–10]. Cyanide is irreversibly adsorbed on Pt single-crystal electrodes: the case of Pt(1 1 1) is particularly interesting, due to the spontaneous formation, upon immersion of Pt(1 1 1) in a cyanide-containing solution, of an ordered $(2\sqrt{3} \times 2\sqrt{3})R30°$ structure [1,4,5] which extends over the whole electrode surface and is composed of hexagonally packed hexagons, each of them containing six cyanide groups adsorbed on top of a hexagon of Pt surface atoms surrounding a free Pt atom. This structure was observed for the first time using low-energy electron diffraction (LEED) by Hubbard and co-workers [1], who demonstrated that the $(2\sqrt{3} \times 2\sqrt{3})R30°$ structure formed by adsorbed cyanide on Pt(1 1 1) resists electrode emersion and transfer into a UHV chamber, which indicates a very strong adsorption. The atomic, real space structure could later be elucidated by electrochemical STM [4,5]. Although most STM experiments were performed in alkaline solutions [4,5], Itaya and co-workers [5] observed the same structure in acidic solutions.

Cyanide adsorption on Pt(1 1 1) has been intensively studied in acidic solutions by Huerta et al. [6–10], who demonstrated, by means of cyclic voltammetry, that cyanide-covered Pt(1 1 1) could be considered as a chemically modified electrode [6]. The cyanide

adlayer on Pt(1 1 1) is remarkably stable, no change being observed upon repetitive cycling between 0.05 and 1.10 V. Cyclic voltammograms (CVs) of cyanide-modified Pt(1 1 1) in $HClO_4$ and in H_2SO_4 solutions are qualitatively very similar, indicating the insensitivity of the chemically modified surface to the anions present in the supporting electrolyte, i.e., adsorbed cyanide acts as a third-body, which selectively blocks the sites necessary for the adsorption of tetrahedral anions, such as sulfate, on Pt, while leaving unaffected the CN-free Pt atoms onto which OH, CO or NO [10–12] can adsorb.

A very appropriate way to study the role of geometric atomic ensembles in electrocatalysis is to modify the surface in such a way that only one kind of site is removed without modifying the electronic structure of the rest of the surface (the site-knockout strategy [13]). Interestingly, all the sites composed of three contiguous Pt atoms are absent on cyanide-modified Pt(1 1 1) and, as a consequence, adsorption at *three-fold hollow* sites [12,14] or reaction steps requiring three contiguous Pt atoms [15,16] are inhibited. These chemically modified surfaces have been used to demonstrate that the dehydrogenation of methanol [15] and the dehydration of formic acid [16] to adsorbed carbon monoxide require at least three contiguous Pt atoms. Furthermore, modification of Pt(1 1 1) with cyanide results in a huge enhancement of the catalytic activity for the ORR in sulfuric and phosphoric acid solutions, because the sites necessary for the adsorption of the tetrahedral anions of these acids have been blocked [14]. In all the previous cases, it was assumed that significant simultaneous electronic effects were absent, although we lacked a clear and definitive proof. Cyanide-modified Pt(1 1 1) surfaces can also be used to study the role of non-covalent interactions at the electrochemical double layer [17],

* Corresponding author.
 E-mail address: a.cuesta@iqfr.csic.es (Á. Cuesta).

and cations non-covalently attached to the electrode surface can be used as precursors for surface nanostructuring [18,19].

Theoretical studies concerning the spatial and electronic structure, as well as the stability of cyanide-modified Pt(1 1 1) surfaces, are needed due to the interest in employing this system to study atomic ensemble effects in electrocatalysis and as a template to fabricate nanostructures on surfaces. Additionally, theoretical calculations are particularly necessary in order to understand the adsorption of hydrogen on cyanide-modified Pt(1 1 1) surfaces. The present contribution addresses these points.

2. Experimental and computational details

Experimental details have been reported previously [11,12,15–18]. Briefly, cyanide-modified Pt(1 1 1) electrodes were prepared by immersion of a clean and well-ordered Pt(1 1 1) surface in a 0.1 M KCN (Merck, p.a.) solution for approximately 3 min, after which the electrode was rinsed with ultrapure water and transferred to the electrochemical or spectroelectrochemical cell containing the cyanide-free solutions. A reversible hydrogen electrode (RHE) and a platinum wire were used as reference and counter electrode, respectively. All the potentials in the text are referred to the RHE.

Calculations were performed either with the DACAPO [20] or with the SIESTA [21] DFT codes. In those cases in which the same calculation was performed with both codes, identical results, within the error margins, were obtained. More computational details can be found in Supporting information.

3. Results and discussion

Although the structure of adsorbed cyanide on Pt(1 1 1) electrodes has been elucidated by LEED [1] and in situ STM [4,5], and although many unique properties of these chemically modified electrodes have been experimentally proved [6–11], there is a lack of theoretical studies concerning the structure and the configuration adopted by adsorbed cyanide on Pt(1 1 1) surfaces. Theoretical calculations are particularly necessary in order to understand (i) the reason why the cyanide adlayer adopts the experimentally observed $(2\sqrt{3} \times 2\sqrt{3})R30°$ structure and (ii) the effect of adsorbed cyanide on the electronic structure of the Pt atoms not directly bonded to CN, and the experimental results regarding the adsorption of hydrogen on cyanide-modified Pt(1 1 1).

3.1. Structure of cyanide adsorbed on Pt(1 1 1) surfaces

In order to study the dependence of the adsorption energy of cyanide on the coverage of CN_{ad}, we have calculated the adsorption energy of CN on Pt(1 1 1) surfaces for different adsorption sites (on-top, bridge, fcc-hollow and hcp-hollow) and various configurations in the coverage interval between 0.25 and 1 ML. The adsorption energy was calculated taking the substrate and the radical adsorbate as reference (Eq. (1)). We have also computed the changes in the work function induced by CN_{ad} on a Pt(1 1 1) surface, given by Eq. (2), where the sub-index adsorbate is referred to CN_{ad}. The calculated work function of the Pt(1 1 1) surface obtained using DACAPO is $\Phi_{Pt(1 1 1)} = 5.80$ eV.

$$E_{ad} = E_{CN–Pt(1 1 1)} - (E_{CN} + E_{Pt(1 1 1)}) \tag{1}$$

$$\Delta\Phi = \Phi_{adsorbate–Pt(1 1 1)} - \Phi_{Pt(1 1 1)} \tag{2}$$

Fig. 1 shows top views of the configurations with CN_{ad} in an on-top position for which E_{ad} of cyanide on Pt(1 1 1) at $\theta_{CN} = 0.25$ (Fig. 1A), $\theta_{CN} = 0.75$ (Fig. 1B), and $\theta_{CN} = 1$ (Fig. 1C) were calculated. Calculations for the same cyanide coverages with all the CNs in bridge, fcc-hollow or hcp-hollow sites were performed with the same

Table 1
Adsorption energy (E_{ad}) and work function difference ($\Delta\Phi$) in eV for different configurations and coverages of the CN adlayer on Pt(1 1 1) surfaces.

$\theta_{adsorbate}$	Adsorption site	$E_{ad(CN)}$ (eV)	$\Delta\Phi_{(CN)}$ (eV)
0.25	top	−3.39	2.75
0.25	fcc	−3.47	1.67
0.50	top (exp.)	−3.17	3.56
0.50	top (zig-zag)	−3.10	3.48
0.50	top (linear)	−3.02	3.48
0.50	fcc (linear)	−3.04	2.09
0.50	top–fcc (mix)	−3.23	3.24
1	top	−2.51	3.82
1	fcc	−2.23	3.33

structures by simply shifting the CN groups to the corresponding adsorption site. It must be noted that none of these theoretical structures has been observed experimentally. For the particular case of 0.5 ML, we have calculated the adsorption energy of cyanide for three different configurations: (i) the experimentally observed $(2\sqrt{3} \times 2\sqrt{3})R30°$ structure (Fig. 2A), labeled top (exp.) in Table 1; (ii) a zig-zag distribution with all the CN groups adsorbed on-top (Fig. 2B), that resulted after relaxation of a linear distribution of cyanide in a 2×2 unit cell, due to the repulsion between the nitrogen atoms of neighboring CN groups; and (iii) a mix structure in which half of the CN groups are adsorbed on-top and the other half are adsorbed on three-fold hollow sites (Fig. 2C), that resulted after relaxation of a 2×2 unit cell in which cyanide was adsorbed in the three-fold hollow (fcc or hcp) sites. The calculated adsorption energies for on-top and fcc-hollow sites corresponding to the configurations illustrated in Figs. 1 and 2 are given in Table 1 (note that the results for $\theta_{CN} = 0.75$, corresponding to the configuration in Fig. 1B, have not been included in Table 1).

The coverage dependence of the calculated adsorption energy of cyanide adsorbed on-top and at fcc-hollow sites is shown in Fig. 3A. Obviously, the adsorption energy becomes less negative as the coverage increases due to the repulsion between adsorbed CN groups. As can be seen in Table 1 and Fig. 3A, the energy difference between different adsorption sites is too small to explain the experimentally observed preference for adsorption on-top, that most likely is due to an additional energy gain by the interaction of the negative charge accumulated on the N atom of the CN moieties with the water dipoles at the interface, which were not included in our calculations.

As shown in Fig. 3A, the calculated adsorption energy curves for fcc and on-top sites intercross at $\theta_{CN} = 0.5$. Fig. 3B shows the calculated total electronic density vs. the distance from the metal surface (z) for CN_{ad} coverages of 0.25 and 1. At $\theta_{CN} = 0.25$, the charge density initially decreases fast with the distance from the surface, and then remains more or less constant until it vanishes at distances longer than the nitrogen-surface separation. In contrast, at $\theta_{CN} = 1$, there is a local maximum at the location of the nitrogen atoms. This electron accumulation is large enough as to produce charge repulsion between the large electronic density of the nitrogen atoms and the electrons of the Pt(1 1 1) surface. Since in the case of CN adsorbed on-top nitrogen atoms are located farther from the surface, the repulsion is lower, and the calculated adsorption energy is slightly lower for on-top sites than for fcc sites. This result suggests that the calculated adsorption energy of CN on Pt(1 1 1) results from a competition between two types of forces: a chemical force, that tends to locate CN_{ad} on the fcc site, and an electrostatic force that tends to push the CN_{ad} further from the surface and favors adsorption on-top. The larger dipole moment induced in the case of CN adsorption on-top at high coverage, due to the larger charge separation (Fig. 3B), will favor the solvation of CN by water molecules, and, as noted above, will contribute to the experimentally observed
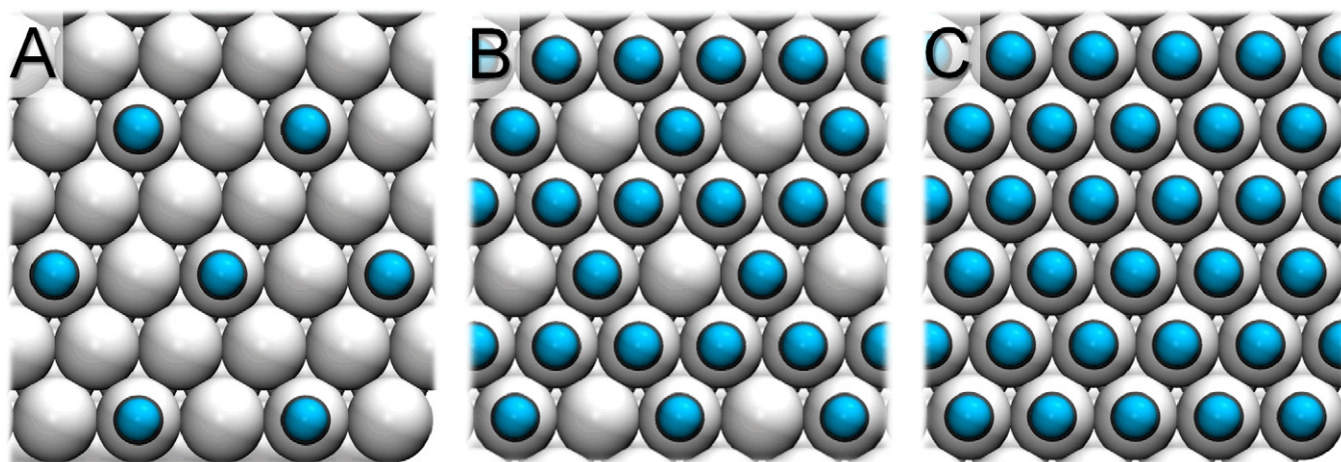
Fig. 1. Top views of the different structures with $\theta_{CN} = 0.25$ (A), $\theta_{CN} = 0.75$ (B), and $\theta_{CN} = 1$ (C) for which the adsorption energy of cyanide adsorbed _on-top_ on Pt(1 1 1) has been calculated.

preference of the CN groups to be adsorbed _on-top_, that, as noted above, cannot be justified based exclusively on our DFT calculations.

For all the structures considered in Table 1 the changes in the work function, $\Delta\Phi_{CN}$, caused by CN adsorption, are large (of the order of a few electron volts) and positive. In an aqueous solution, the large dipole moment of the adsorbed CN groups will induce a net orientation of the water dipoles in the opposite direction, which will partially cancel the surface dipole potential. To get an idea of the magnitude at which the surface dipole may be compensated by

the solvent orientation, we can recall the results obtained by one of us [22], who found, for the case of sp metals, a contribution of the solvent to the potential drop across the interface between −0.2 and −0.4 V. These results were confirmed later using semiempirical models for the metal [23] and, in the case of Ag, the solvent contribution was predicted to be of the order of −0.6 V [24], in agreement with experimental work function measurements [25]. More recently, one of us has determined experimentally, for the case of Pt(1 1 1) and CO-covered Pt(1 1 1) electrodes in 0.1 M HClO$_4$,
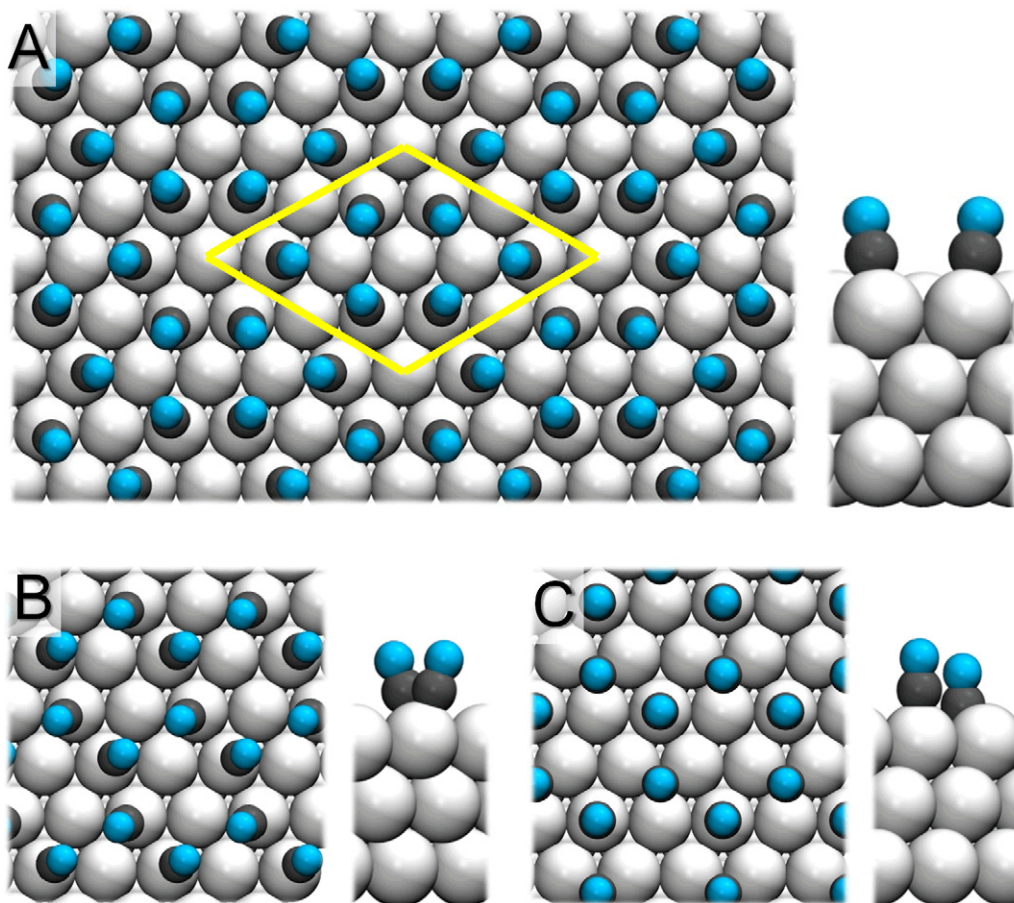

Fig. 2. Top and side views of the structures with $\theta_{CN} = 0.5$ for which the adsorption energy of cyanide on Pt(1 1 1) has been calculated: (A) experimentally observed $(2\sqrt{3} \times 2\sqrt{3})R30°$ structure; (B) (2×2) _zig-zag_ structure; (C) (2×2) _mix_ structure.
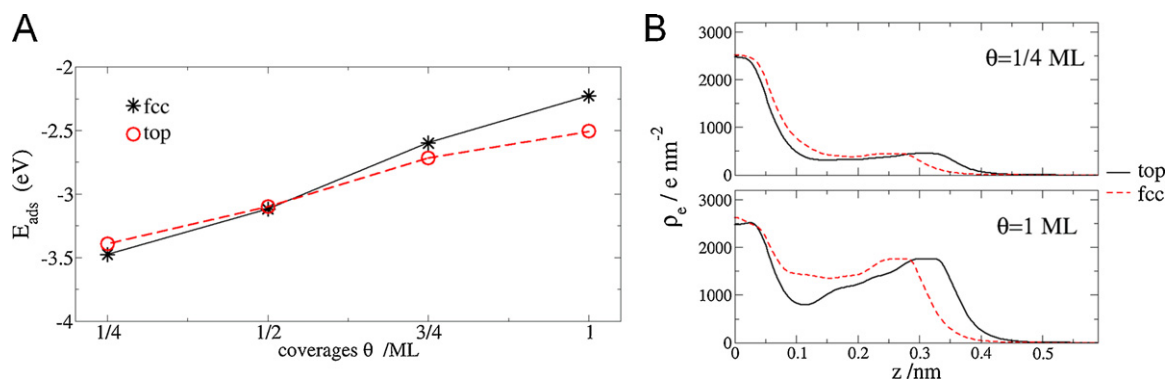
Fig. 3. (A) Adsorption energy of CN_{ad} on Pt(1 1 1) at different coverages from 0.25 to 1 ML, with all the CNs occupying either *fcc-hollow* sites (black stars) or *on-top* sites (red circles) and adopting the structures shown in Fig. 1. (B) Total electronic density (ρ_e) as a function of the distance (z) from the metal surface for cyanide-modified Pt(1 1 1). The Pt surface corresponds to $z = 0$. The total charge density for adlayers with all the CNs at *fcc-hollow* and at *on-top* sites are compared for $\theta_{CN} = 0.25$ (top) and $\theta_{CN} = 1$ (bottom). (For interpretation of the references to color in this figure legend, the reader is referred to the web version of the article.)

Table 2
Adsorption energies, relevant structural parameters, and Mulliken charge analysis for the three possible structures for Na^+ and K^+ adsorbed on the CN-modified Pt(1 1 1) surface.

Structure	E_{ad} (eV)[a]	$d(M^+–Pt)$ (nm)[b]	$d(N–M^+)$ (nm)[c]	$d(N–Pt)$ (nm)[d]	δ_{M+} (e)[e]	δ_{CN} (e)[e]
M = Na						
Kagome	−5.31	0.369	0.259	0.314	+0.88	−0.42
Honeycomb	−5.59	0.423	0.243	0.314	+0.88	−0.32
$(CN_{ad})_6–Na^+$	−5.35	0.391	0.322	0.319	+0.90	−0.22
M = K						
Kagome	−5.42	0.386	0.265	0.314	+0.85	−0.40
Honeycomb	−5.62	0.444	0.261	0.314	+0.90	−0.32
$(CN_{ad})_6–K^+$	−5.82	0.445	0.275	0.319	+0.90	−0.24

[a] Adsorption energy referred to the optimized $(2\sqrt{3} \times 2\sqrt{3})R30°$ CN adlayer and a M atom in the vacuum.
[b] Distance between the cation and the Pt surface in the optimized structure.
[c] Average distance between M^+ and the N atom of the CN groups surrounding the adsorption site.
[d] Average distance from the N atoms of the adsorbed CN groups to the Pt surface.
[e] Mulliken charge of the species in the optimized structure.

the contribution at the pzc of the interfacial water layer to the potential drop across the interface [26], that was found to be of −1.07 V in the case of Pt(1 1 1) and of −0.2 V in the case of Pt(1 1 1) covered by a saturated CO adlayer. Nevertheless, in the present case, a net increase of the work function should result, entailing a concomitant shift of the potential of zero charge (pzc) to more positive values. Therefore, the adsorption of cations will set in at more positive electrode potentials than at the bare Pt(1 1 1) electrodes. The larger changes in the work function upon adsorption of cyanide when *on-top* sites are occupied at different CN coverages, including the $(2\sqrt{3} \times 2\sqrt{3})R30°$ structure observed experimentally, as compared with CN adsorbed on *fcc-hollow* sites, are also due to the larger dipole moment of CN_{ad} in the former case.

As can be seen in Fig. 2A, a pseudohexagonal arrangement of the adsorbed cyanide groups results after relaxation of the experimentally observed $(2\sqrt{3} \times 2\sqrt{3})R30°$ structure of cyanide-modified Pt(1 1 1), due to the tendency of the nitrogen atoms to be as far from each other as possible, causing the CN groups not to be perpendicular to the metal surface. The adsorption energy calculated for the relaxed $(2\sqrt{3} \times 2\sqrt{3})R30°$ structure is −3.17 eV (Table 1), and is very close in energy to the other two alternative configurations with the same θ_{CN} (Table 1): the *zig-zag* distribution, shown in Fig. 2B (E_{ad} = −3.10 eV), and the *mix* structure (Fig. 2C, E_{ad} = −3.23 eV). The slightly higher stability of the latter structure is mainly due to the location of the CN groups at different heights above the metal surface (Fig. 2C), which lowers the repulsion between the N atoms of two neighboring CN groups. These results indicate that, from a thermodynamical point of view, equilibrium between the three structures described above should be expected. However, as indicated above, only the $(2\sqrt{3} \times 2\sqrt{3})$ structure has been

experimentally observed. A cation located at the center of each hexagonal cyanide ring of the $(2\sqrt{3} \times 2\sqrt{3})$ structure, as suggested by Itaya and co-workers based on their STM images [5] in solutions containing K^+ or Na^+, could explain the tendency of CN_{ad} to form an ordered array of hexagons, instead of distributing themselves over the surface with a homogeneous CN–CN separation. However, according to our DFT calculations of the adsorption energy of alkaline metal cations (approximated as neutral metals) on different adsorption sites (Table 2), the center of the CN hexagonal rings (one adsorbed cation per unit cell, Fig. 4A) is the most favorable site in the case of K, but adsorption at the $(CN)_3$ sites (honeycomb structure, Fig. 4B) is the most favorable in the case of Na. In both cases, adsorption at the $(CN)_4$ sites (Fig. 4C, kagome structure) is the least favorable. (A kagome lattice is an arrangement of lines composed of interlaced triangles, such that each point where two lines cross has four neighboring similar crossing points. See, e.g., Figs. 4C and 5.) We would like to note here that, in the first-principles calculations method that we have used, no particular assumption is made on the status of charge of the cations. In this way, they acquire the charge determined by the energy minimization of the energy functional with respect to the electronic density. In this respect, it is interesting to point out that the cations do take, as chemical intuition dictates, a large positive charge, as can be noted in the sixth column of Table 2.

In any case, we have strong grounds to affirm that cations, which are always present during the experimental formation of the cyanide adlayer, may play an important role in determining the structure of cyanide-modified Pt(1 1 1) electrodes. Experimental evidence of the presence of cations attached to the cyanide-modified Pt(1 1 1) has been reported even under UHV conditions
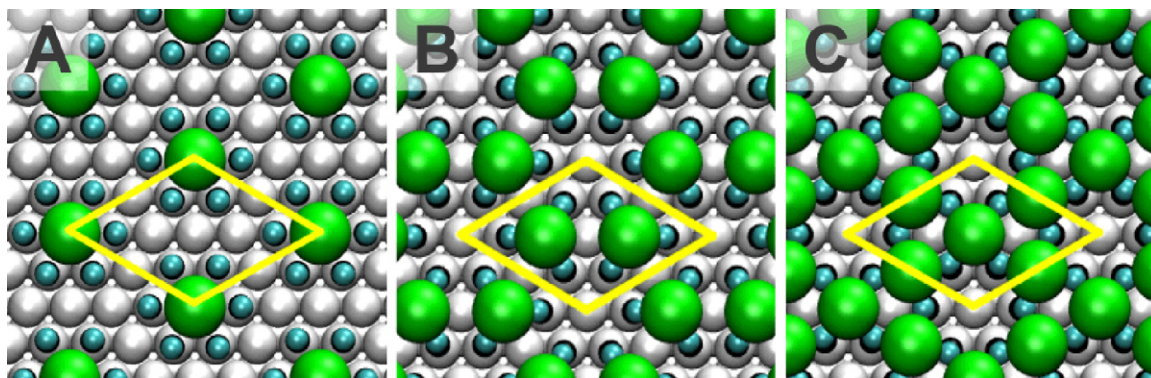
Fig. 4. Top view of the three possible cavity sites at which cations can adsorb on the experimentally observed $(2\sqrt{3} \times 2\sqrt{3})R30°$ structure of cyanide-modified Pt(1 1 1) surfaces: (A) $(CN_{ad})_6$, (B) $(CN_{ad})_3$ and (C) $(CN_{ad})_4$ cavities.

by ex situ LEED experiments [1]. Our recent quantitative study of non-covalent interactions between alkali-metal cations and the CN groups of cyanide-modified Pt(1 1 1) electrodes has shown that a good match between the size of the cation and that of the cavity in which it has to be accommodated is critical in determining the cation's adsorption energy [17]. A comparison of the *zig-zag* and the *mix* structures with the $(2\sqrt{3} \times 2\sqrt{3})$ structure suggests that the size of the different cavities available for the adsorption of cations plays a crucial role in determining the optimized configuration. The *mix top-fcc* arrangement, which is the most stable according to the theoretical calculations, does not seem a stable candidate for the adsorption of cations due to the large size of the cavity formed by a trigonal arrangement of Pt atoms. As for the *zig-zag* structure, although the cavity in this case is quite similar to that of the experimentally observed structure, in the presence of counter-ions the CN groups probably tend to rearrange, rendering a distribution less stable than the $(2\sqrt{3} \times 2\sqrt{3})$ structure.

3.2. Hydrogen adsorption on cyanide-modified Pt(1 1 1) surfaces

The double layer-corrected voltammetric charge in the hydrogen adsorption region of a cyanide-modified Pt(1 1 1) electrode amounts to ca. 80 μC cm^{-2}, which is the charge expected for the adsorption of atomic hydrogen on two thirds of the Pt atoms left free upon modification of the Pt(1 1 1) electrode with cyanide, in very good agreement with Huerta et al. [7], who suggested that adsorbed cyanide blocks only some of the sites available for hydrogen adsorption. Interestingly, on cyanide-modified Pt(1 1 1) the

onset of hydrogen adsorption is shifted positively by ca. 0.20 V with respect to unmodified Pt(1 1 1) electrodes (Fig. S1). This implies that ΔG_0 of H_{upd} ($\theta_H = 0$) is ca. 19 kJ mol^{-1} more negative on cyanide-modified Pt(1 1 1) [12], and might suggest a modification of the electronic structure of the free Pt atoms in the cyanide-modified Pt(1 1 1) surface. As we will show below, this is not the case. Actually, the onset of hydrogen evolution does not seem to be affected by the presence of CN_{ad} on cyanide-modified Pt(1 1 1) electrodes (Fig. S1), onto which *on-top* sites, thought to be the active ones in the evolution of H_2 on Pt(1 1 1) electrodes, are perfectly available. If these sites remain electronically unaltered, hydrogen evolution would be expected to coincide on both Pt(1 1 1) and cyanide-modified Pt(1 1 1) electrodes.

The shift in the onset of hydrogen adsorption can be explained by the formation in the H_{upd} region of adsorbed hydrogen isocyanide, CNH_{ad}, instead of H_{ad} directly bonded to the Pt atoms. This idea had been already proposed by Schardt et al. [27], who suggested that the CNH_{ad} adlayer behaves as a polyprotic acid. The formation of $(CN_{ad})_x$—H (with x decreasing with decreasing potential within the H adsorption region) would explain all the previous experimental facts. As can be observed in Fig. 5, the charge density at the broad peak at 0.48 V in the H_{upd} region is ca. 20 μC cm^{-2} ($\theta_{CNH} = 1/12$ ML), which might correspond to a $(CN_{ad})_6$—H stoichiometry. The minimum of current density at ca. 0.40 V corresponds to a charge density of about 32 μC cm^{-2} ($\theta_{CNH} = 1/8$ ML), coinciding with the charge expected for the formation of $(CN_{ad})_4$—H. Finally, at 0.37 V and ca. 0.20 V, the charge densities are 40 μC cm^{-2} ($\theta_{CNH} = 1/6$ ML) and 64 μC cm^{-2} ($\theta_{CNH} = 0.25$ ML), respectively. The former may
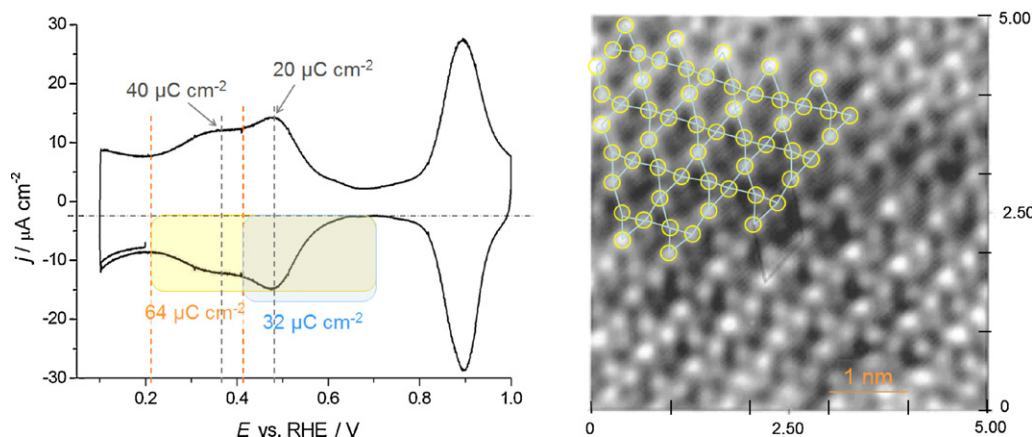

Fig. 5. Left: Cyclic voltammogram at 50 mV s^{-1} of cyanide-modified Pt(1 1 1) in 0.1 M HClO$_4$. Right: 5 × 5 nm^2 STM image obtained at 0.3 V, reprinted and adapted with permission from Ref. [9], copyright 1996 American Chemical Society. The image can be interpreted as a kagome structure corresponding to a $(CN_{ad})_2$—H stoichiometry.

correspond to a $(CN_{ad})_3$—H stoichiometry (honeycomb structure), and the latter to a $(CN_{ad})_2$—H stoichiometry (kagome structure).

Itaya and co-workers [5] attributed the STM images of a cyanide-modified Pt(1 1 1) electrode obtained at 0.30 V vs. RHE (well within the H_{upd} region) in perchloric acid solutions to a $(\sqrt{7} \times \sqrt{7})R19°$ structure, but this is in contradiction with the absence in the cyclic voltammogram of any feature indicating a phase transition, as would be expected for a change from a long-range ordered $(2\sqrt{3} \times 2\sqrt{3})R30°$ structure to a long-range ordered $(\sqrt{7} \times \sqrt{7})R19°$ structure. As shown in Fig. 5, the structure found by Itaya and co-workers can also be interpreted as a kagome structure, in excellent agreement with our analysis above, based on the charge density measured in the corresponding CV.

The IR spectra of cyanide adsorbed on Pt(1 1 1) electrodes have been intensively studied both in acidic [6,7] and in alkaline solutions [3,4,28,29]. The spectra show a single vibrational band corresponding to the stretching vibration of a CN group adsorbed *on-top* of a platinum atom through its carbon atom (CN_L) [3,4,6,7]. A plot of the CN_L stretching frequency of cyanide-modified Pt(1 1 1) vs. the electrode potential (Fig. S2) shows two clearly different slopes: at $E \leq 0.5$ V the CN_L stretching frequency increases with potential with a slope of 82 cm^{-1} V^{-1}, this being significantly smaller than that of ca. 100 cm^{-1} V^{-1} reported by Huerta et al. [6,7], while for $E \geq 0.60$ V the slope is 25 cm^{-1} V^{-1}, in good agreement with the literature [6,7]. Some authors attributed this change in the Stark tuning rate to a change from N-bound CN at $E \leq 0.50$ V to C-bound CN at $E > 0.50$ V [6,7,30], and this assignment was supported by theoretical calculations of Pt—CN$^-$ and Pt—NC$^-$ vibrational systems [31,32]. In contrast, Paulissen and Korzeniewski [2] suggested that the changes in the Stark tuning rate correspond to the conversion from Pt—CN to Pt—CNH species. Naturally, due to bond order conservation, the adsorption of hydrogen on the nitrogen atoms of adsorbed cyanide should weaken the carbon—nitrogen bond, and hence decrease the corresponding C—N stretching vibrational frequency. A comparison of the plot of the CN_L stretching frequency of cyanide-modified Pt(1 1 1) vs. the electrode potential (Fig. S2) with the CV of the cyanide-modified Pt(1 1 1) electrode (Fig. S1) strongly suggests that the high slope at $E \leq 0.50$ V must be due to the presence of hydrogen protonating the nitrogen atoms of the adsorbed cyanide. Therefore, our hypothesis is that over the whole frequency range between 2085 and 2123 cm^{-1} the band of the cyanide-modified Pt(1 1 1) corresponds to C-bound CN adsorbed on-top on Pt(1 1 1) and that the change in the Stark tuning rate of the CN stretching frequency at ca. 0.50 V, coinciding with the onset of hydrogen adsorption in the cyclic voltammogram, can be explained by the formation of $(CN_{ad})_x$—H.

We have analyzed the projected density of states (PDOS) of the topmost Pt atoms, in order to identify the electronic factors that control the adsorption of CN on Pt(1 1 1) surfaces, and in order to prove our assumption that the electronic structure of the surface Pt atoms that are not directly bonded to CN remains essentially unaltered. Fig. 6A shows the DOS projected on the carbon atom of a CN_{ad} and on the Pt atom of the cyanide-modified Pt(1 1 1) surface bonded to it. As can be observed there is a resonance of Pt/CN states at around −16 eV, where the 2sp states of carbon and the 6sp states of platinum clearly overlap. A contribution of the d states of Pt can also be detected at around −7.5 eV.

The DOS projected on the *d*-band of the surface Pt atoms of a cyanide-modified Pt(1 1 1) electrode with the $(2\sqrt{3} \times 2\sqrt{3})R30°$ structure (Fig. 6B), shows that the PDOS of the Pt atoms directly bonded to the CN_{ad} is shifted to lower energies as compared to clean Pt(1 1 1), this being consistent with a strong bonding. On the other hand, the DOS projected on the *d*-band of the free Pt atoms remains nearly identical to the PDOS of the Pt atoms of the clean (1 1 1) surface, supporting the notion that CN_{ad} acts as an inert site

Table 3

Adsorption energy (E_{ad}), distance of the adsorbed H to the surface and Mulliken charge on the adsorbed H atom ($\theta_H = 1/9$) for the different adsorption sites on Pt(1 1 1).

Adsorption site	E_{ad} (eV)	d(H—Pt) (nm)	Mulliken charge on H
top	−0.54	0.159	−0.22
bridge	−0.58	0.105	−0.28
hollow-fcc	−0.63	0.088	−0.27
hollow-hcp	−0.59	0.089	−0.27

blocker. Hence, the positive shift in the onset potential for hydrogen adsorption cannot be explained by an electronic disturbance of the free Pt atoms of the cyanide-modified Pt(1 1 1) surface.

As a first approximation, we calculated the adsorption energies at low coverage (1/9 ML) of the CN radical (Eq. (1)) and of H (Eq. (3)) onto a clean Pt(1 1 1) surface and of H onto a Pt(1 1 1) surface with a low coverage of adsorbed CN ($\theta = 1/9$ both for H and for CN), both on a free Pt atom (Eq. (4)) and protonating the N atom of a CN group (Eq. (5)). Fig. 7 illustrates the low-coverage structures for which these calculations where performed, Table 3 summarizes the relevant information concerning the adsorption of H onto a clean Pt(1 1 1) surface, and Table 4 that for the adsorption of CN and for the adsorption of H onto a Pt(1 1 1) surface with 1/9 ML of CN. The adsorption energies for H are calculated with respect to a H_2 molecule (Eqs. (3)–(5)).

$$E_{ad}^{H-Pt} = E_{H-Pt(1 1 1)} - \left(\frac{E_{H_2}}{2} + E_{Pt(1 1 1)} \right) \qquad (3)$$

$$E_{ad}^{H-Pt} = E_{H-Pt(1 1 1)-CN} - \left(\frac{E_{H_2}}{2} + E_{NC-Pt(1 1 1)} \right) \qquad (4)$$

$$E_{ad}^{H-NC-Pt} = E_{H-NC-Pt(1 1 1)} - \left(\frac{E_{H_2}}{2} + E_{NC-Pt(1 1 1)} \right) \qquad (5)$$

The adsorption energy of CNH on Pt(1 1 1) is calculated according to Eq. (6):

$$E_{ad} = E_{CNH-Pt(1 1 1)} - (E_{CNH} + E_{Pt(1 1 1)}) \qquad (6)$$

The CN adsorption energies in Table 4 are consistent with those shown in Table 1, although the latter were calculated with DACAPO and the former with SIESTA. Interestingly, the energy of adsorption of hydrogen on the free Pt atoms of a Pt(1 1 1) surface with a low coverage of CN (Table 4 and Fig. 7C) is similar to that on the different sites of a clean Pt(1 1 1) surface (Table 3 and Fig. 7A), and nearly half the energy corresponding to the protonation of the nitrogen atom of Pt(1 1 1)—CN to form Pt(1 1 1)—CNH (Table 4 and Fig. 7B). This is in agreement with the result of the PDOS in Fig. 6 and with our hypothesis that the shift of 0.2 V in the onset of hydrogen adsorption on cyanide-modified Pt(1 1 1), as compared to clean Pt(1 1 1), is due to the formation of CNH_{ad}.

We have also studied the adsorption energy of CNH on Pt(1 1 1), given by Eq. (6), at different coverages, and have compared it with the adsorption energy of CN on Pt(1 1 1), given by Eq. (1). We have also computed the changes in the work function induced by CNH_{ad} on a Pt(1 1 1) surface using Eq. (2), where the sub-index *adsorbate* is now referred to CNH_{ad}. The results of these calculations are shown in Table 5.

The value for the adsorption energy of 0.25 ML of CNH on Pt(1 1 1) in Table 5 is in very good agreement with the value obtained for 0.19 ML of CNH in Table 4, although the former was obtained with DACAPO and the latter with SIESTA. Table 5 shows that the adsorption of CNH_{ad} inverts the dipole moment of the surface with respect to CN_{ad} (Table 1). As happens with CN_{ad}, large differences in the work function changes are found for CNH_{ad} in the different configurations studied, in contrast with the small change in the adsorption energy found for the same coverages of CNH_{ad}
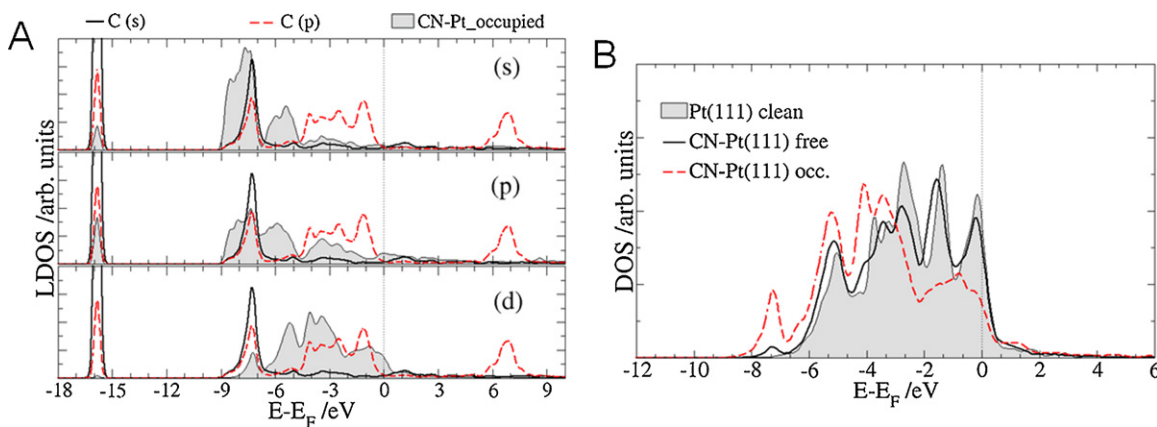
Fig. 6. (A) DOS projected on the C atom of a CN$_{ads}$ group of the $(2\sqrt{3} \times 2\sqrt{3})R30°$ structure and on the Pt atom bonded to it. The sp states of carbon are contrasted with, from top to bottom, the s, p, and d valence states of the metal. (B) DOS of the *d*-band projected on the surface atoms of a clean Pt(1 1 1) and of a cyanide-modified Pt(1 1 1) surface with the experimentally observed $(2\sqrt{3} \times 2\sqrt{3})R30°$ structure. For the cyanide-modified Pt(1 1 1) surface, Pt free atoms (not bonded to adsorbed cyanide) are distinguished from the Pt atoms directly bonded to CN (Pt occupied).
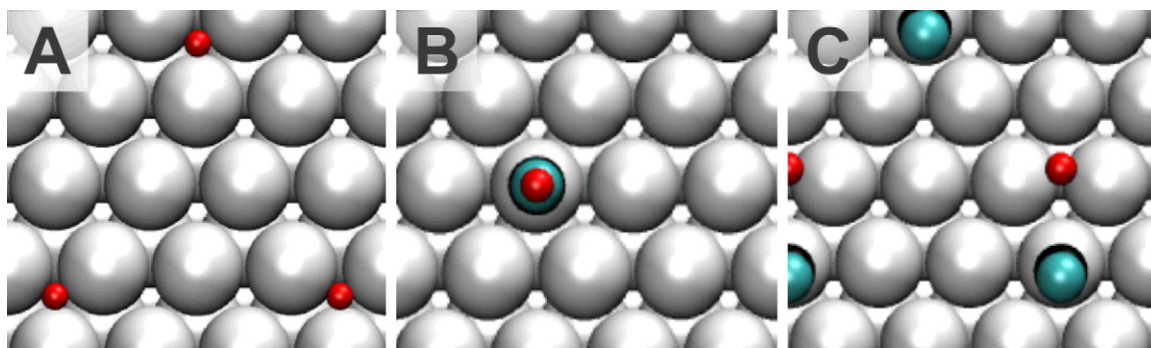
Fig. 7. (A) H adsorbed on a *hollow fcc* site on Pt(1 1 1). (B) CN adsorbed *on top* protonated on the N atom. (C) CN adsorbed *on top* and H adsorbed at a site intermediate between *bridge* and *hcp-hollow*, resulting from the relaxation of a structure in which H was originally adsorbed at one of the *fcc-hollow* sites adjacent to the adsorbed CN group.

Table 4

Adsorption energy (E_{ad}), structural parameters and Mulliken charges for the CN radical adsorbed *on-top* on Pt(1 1 1) at low coverage, and for the H atom adsorbed on the nitrogen atom of the CN (Pt(1 1 1)—CNH) and at a Pt site intermediate between *bridge* and *hcp-hollow* (NC—Pt(1 1 1)—H) in the presence of a low coverage of CN$_{ad}$.

Structure	E_{ad} (eV)		Atomic distances (nm)			Mulliken charges	
Pt(1 1 1)—CN[a]	CN: −3.59		Pt—C: 0.194	C—N: 0.120		CN: −0.20	
Pt(1 1 1)—CNH[b]	CNH: −1.86	H: −0.92	Pt—C: 0.189	C—N: 0.119	N—H: 0.101	CN: +0.38	H: −0.14
NC—Pt(1 1 1)—H[c]	CN: −3.54	H: −0.55	Pt—C: 0.194	C—N: 0.120	Pt—H: 0.100	CN: −0.23	H: −0.20

[a] CN adsorbed *on-top* of a Pt(1 1 1) atom, $\theta = 1/9$.

[b] CNH adsorbed *on-top* of a Pt(1 1 1) atom, $\theta = 1/9$ (Fig. 7B); the value given for CNH in column two corresponds to the E_{ad} of a CNH molecule on Pt(1 1 1) calculated with Eq. (6), while the value given for H corresponds to E_{ad} of a H atom on the N atom of an adsorbed CN moiety calculated with Eq. (5).

[c] CN and H adsorbed *on-top* and on a site intermediate between *bridge* and *hcp-hollow*, respectively (Fig. 7C); the value given for CN in column two corresponds to the E_{ad} of a CN radical on Pt(1 1 1) calculated with Eq. (1), while the value given for H corresponds to E_{ad} of a H atom on a CN-free Pt atom ($\theta_H = 1/9$) of a Pt(1 1 1) surface covered by 1/9 ML of CN, calculated with Eq. (4).

Table 5

Adsorption energy (E_{ad}) and work function difference ($\Delta\Phi$) in eV for different configurations and coverages of a CNH adlayer on Pt(1 1 1) surfaces.

$\theta_{adsorbate}$	Adsorption site	$E_{ad(CNH)}$ (eV)	$\Delta\Phi_{(CNH)}$ (eV)
0.25	*top*	−1.86	−2.66
0.25	*fcc*	−2.11	−0.88
0.50	*top (zig-zag)*	−1.43	−3.37
0.50	*top (linear)*	−1.60	−2.23
0.50	*fcc (linear)*	−1.81	−0.86
0.50	*top-fcc (mix)*	−1.87	−2.38
1	*top*	−1.04	−2.69
1	*fcc*	−0.96	−1.63

(Table 5). The positive values calculated for $\Delta\Phi_{(CNH)}$ using DACAPO (Table 5) are in agreement with the positive total charge on the CNH$_{ad}$ species inferred from the Mulliken analysis, obtained using SIESTA, in Table 4.

The adsorption energy of hydrogen on Pt(1 1 1) covered by CN with $\theta_{CN} = 0.25$ (Figs. 8A, B and 9A, B) and $\theta_{CN} = 0.5$ (Figs. 8C, D and 9C, D), both on the nitrogen atom of adsorbed cyanide (Fig. 8) and on the Pt atoms of the Pt(1 1 1) surface (Fig. 9), was also calculated according to Eqs. (5) and (7). The results are summarized in Table 6. Although the *zig-zag* arrangement is one of the most stable configurations for 0.5 ML of CN on Pt(1 1 1), as can be observed in Table 1, for CNH$_{ad}$ it becomes unfavorable, because the CNH groups rearrange in a linear configuration in order to favor the formation of hydrogen bonds between neighboring adsorbates (Fig. 8C and D), that add additional stability to the adlayer and cannot be formed in the *zig-zag* configuration. It must be noted
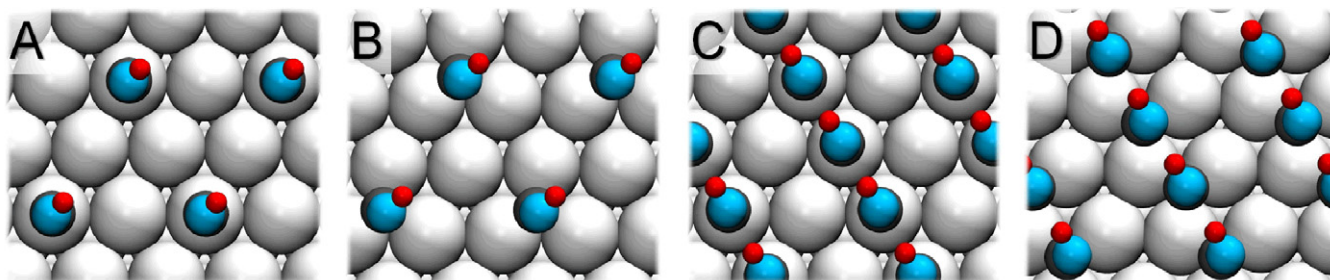
Fig. 8. Top view of the different configurations for which the adsorption energy of hydrogen on the nitrogen atoms of CN_{ad} of CN—Pt(1 1 1) surfaces has been calculated.

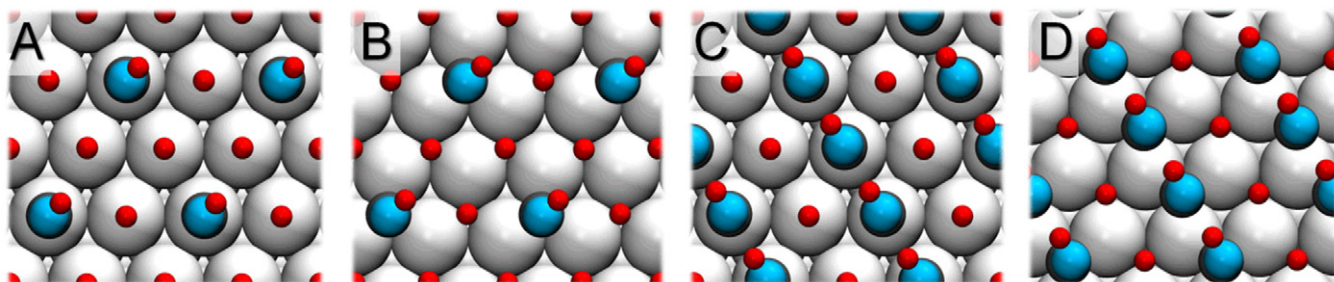**Fig. 9.** Top view of the different configurations for which the adsorption energy of hydrogen on the free Pt atoms of CNH—Pt(1 1 1) surfaces has been calculated.

that the values of E_{ad}^{H-Pt} shown in Table 6 and calculated with Eq. (7) correspond to the adsorption of H on the free Pt atoms of Pt(1 1 1)—CNH_{ad}, when hydrogen is already adsorbed on the nitrogen atom of the CN groups. We have checked that the difference of these results with respect to E_{ad}^{H-Pt} on Pt(1 1 1)—CN_{ad}, i.e., when H is not bonded to the nitrogen atom of the CN groups, is negligible (lower than 0.1 eV). This is confirmed by the similitude between the energy of adsorption of H on a free Pt atom in Tables 4 and 6, although in the former case the calculation was performed with SIESTA and in the latter with DACAPO, and despite the differences in θ_{CN} and θ_H.

$$E_{ad}^{H-Pt} = E_{HNC-HPt(1 1 1)} - \left(\frac{E_{H_2}}{2} + E_{HNC-Pt(1 1 1)} \right) \qquad (7)$$

Although none of the structures for which E_{ad}^{H-Pt} was calculated in Table 6 corresponds to the experimentally observed $(2\sqrt{3} \times 2\sqrt{3})$ structure, the results corroborate that the adsorption of hydrogen on the free Pt atoms of the different structures of cyanide-modified Pt(1 1 1) is very close in energy to the adsorption on unmodified Pt(1 1 1), as already deduced from the results of the calculation of the d-band PDOS (Fig. 6) and from the results in Table 4. These results show that hydrogen adsorbed on the nitrogen atom of CN_{ad} is between ca. 0.5 and ca. 1 eV more stable than hydrogen adsorbed on the free Pt atoms of the cyanide-modified Pt(1 1 1) surface, and strongly support the hypothesis that the hydrogen adsorption region on cyanide-modified Pt(1 1 1) is due to the formation of $(CN_{ad})_x$—H.

In addition to the calculations above, that involve surface structures not observed experimentally, the adsorption of H onto the experimentally observed Pt—CN $(2\sqrt{3} \times 2\sqrt{3})R30°$ surface was also investigated, both in the presence and in the absence of a competing species such as K. The adsorption of H onto the free Pt atoms of a Pt—CN $(2\sqrt{3} \times 2\sqrt{3})R30°$ surface was studied at a low coverage ($\theta = 1/12$) of H, because the onset of hydrogen adsorption, for which a positive shift of 0.20 V is observed in the case of cyanide-modified Pt(1 1 1), corresponds to the limit of zero coverage. The different possible adsorption modes that were assessed include H on *top* of the free Pt atoms considering the three different possible sites: (i) Pt—$(CN)_3$, a free Pt with 3 first neighbors with a CN_{ad} (Fig. 10A); (ii) Pt—$(CN)_4$, a free Pt with 4 first neighbors with a CN_{ad} (Fig. 10B); and (iii) Pt—$(CN)_6$, a free Pt with 6 first neighbors with a CN_{ad} (Fig. 10C). We also tried to adsorb H on hollow sites. On the Pt—CN $(2\sqrt{3} \times 2\sqrt{3})R30°$ surface there are no hollow sites surrounded by three free Pt atoms, but it contains hollow sites composed of either 2 free Pt and 1 Pt—CN_{ad} or 1 free Pt and 2 Pt—CN_{ad}. When an H atom was placed on one of these hollow sites, we observed two different behaviors: the H atom left the surface, and it either protonated a N atom or a C atom. In the latter case, the resulting HCN molecule desorbed from the surface.

We also studied H adsorption at the N atoms of the CN_{ad} of a Pt—CN $(2\sqrt{3} \times 2\sqrt{3})R30°$ surface, varying the H coverage between 1/12 (Pt—CN—Hx1, Fig. 10D) and 1/4 (with respect to the surface Pt atoms). For $\theta = 1/4$, two different stable structures were found, which we have called Pt—CN—Hx3 geom-1 (Fig. 10E) and Pt—CN—Hx3 geom-2 (Fig. 10F). Finally, H adsorption on top of the

Table 6
Adsorption energy and work function difference in eV for H adsorbed on N (H—N) or on the Pt surface (H—Pt) forming different configurations and coverages on Pt(1 1 1) surfaces.

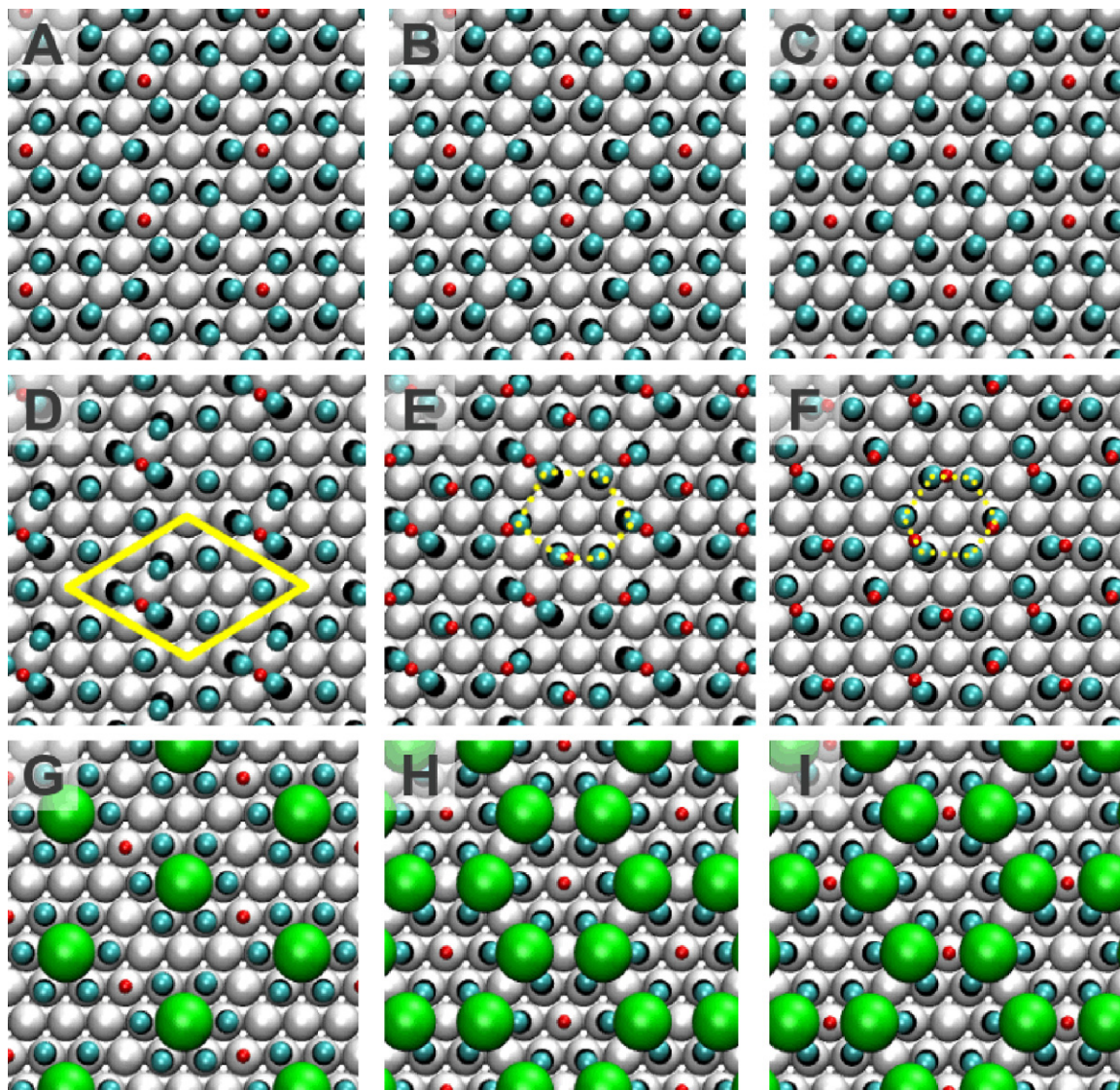| $\theta_{adsorbate}$	Adsorption site	E_{ad}^{H-N} (eV)	E_{ad}^{H-Pt} (eV)	$\Delta\Phi_{(H-N)}$ (eV)	$\Delta\Phi_{(H-Pt)}$ (eV)
0.25	*top*	−1.10	−0.31	−2.66	−2.84
0.25	*fcc*	−1.26	−0.33	−0.68	−1.16
0.50	*top (linear)*	−0.95	−0.40	−2.23	−2.33
0.50	*fcc (linear)*	−1.31	−0.28	−0.86	−0.90
0.50	*top-fcc (mix)*	−1.26	–	–	–

Fig. 10. Hydrogen adsorption on the experimentally observed $(2\sqrt{3} \times 2\sqrt{3})R30°$ structure of cyanide-modified Pt(1 1 1) surfaces. (A) Pt—(CN)$_3$—H, H$_{upd}$ on top of free Pt with 3 first neighbors Pt—CN$_{ad}$. (B) Pt—(CN)$_4$—H, H$_{upd}$ on top of free Pt with 4 first neighbors Pt—CN$_{ad}$. (C) Pt—(CN)$_6$—H, H$_{upd}$ on top of free Pt with 6 first neighbors Pt—CN$_{ad}$. (D) Pt—CN—Hx1, H protonating the N atom of the CN adlayer with $\theta = 1/12$. (E) Pt—CN—Hx3 geom-1, H protonating the N atom of the CN adlayer with $\theta = 1/4$. The red hexagon indicates the CN ring, that has deformed as one CN$_{ad}$ has shifted from an *on-top* to a *bridge* position. (F) Pt—CNHx3 geom-2, H protonating the N atom of the CN adlayer with $\theta = 1/4$. G) Pt—CN—K(*center*)—H(CN$_4$), H$_{upd}$ on a free Pt at a Pt—CN$_4$ site in the presence of a K adlayer with the cation located at center of the CN ring. (H) Pt—CN—K(*honeycomb*)—H(CN$_6$), H$_{upd}$ on a free Pt at a Pt—CN$_6$ site in the presence of a K honeycomb adlayer and (I) Pt—CN—K(*honeycomb*)—H(CN$_4$), H$_{upd}$ on a free Pt at a Pt—CN$_4$ site in the presence of a K honeycomb adlayer. (For interpretation of the references to color in this figure legend, the reader is referred to the web version of the article.)

Table 7
Hydrogen and potassium adsorption energy on the $(2\sqrt{3} \times 2\sqrt{3})R30°$ cyanide-modified Pt(1 1 1) surface (E_{ad}), structural parameters and Mulliken charges for the structures illustrated in Fig. 10.

Structure	E_{ad} (eV)		Atomic distances (nm)		Mulliken charges
H$_{upd}$					
Pt—(CN)$_6$—H	H$_{upd}$: −0.42		H—Pt: 0.159		H: −0.11; CN: −0.20
Pt—(CN)$_4$—H	H$_{upd}$: −0.33		H—Pt: 0.159		H: −0.02; CN: +0.38
Pt—(CN)$_3$—H	H$_{upd}$: −0.36		H—Pt: 0.160		H: −0.03; CN: −0.23
Pt—CN—K(*honeycomb*)—H(CN$_6$)	H$_{upd}$: −0.38	K: −5.60	H—Pt: 0.159	K—Pt: 0.445	H: −0.13; CN: −0.14; K: +0.90
Pt—CN—K(*honeycomb*)—H(CN$_4$)	H$_{upd}$: −0.30	K: −5.60	H—Pt: 0.159	K—Pt: 0.446	H: −0.12; CN: −0.33; K: +0.90
Pt—CN—K(*center*)—H(CN$_4$)	H$_{upd}$: −0.49	K: −5.98	H—Pt: 0.159	K—Pt: 0.393	H: −0.06; CN: −0.22; K: 0.86
H protonating CN					
Pt—CN—Hx1	H: −2.28		H—N: 0.113		H: −0.15; CN(H): +0.25; CN···(H): −0.03; CN: −0.18[a]
Pt—CN—Hx3 geom-1	H: −1.94		H—N: 0.108		H: −0.11; CN(H): +0.10; CN: −0.10
Pt—CN—Hx3 geom-1	H: −1.73		H—N: 0.105		H: −0.09; CN(H): +0.10 CN: −0.23

[a] CN(H) stands for protonated CN$_{ad}$, CN···(H) stands for the CN that makes a H-bond with the adsorbed H atoms, and CN are the remaining CN$_{ad}$, that are not involved in the bonding with the H atom.
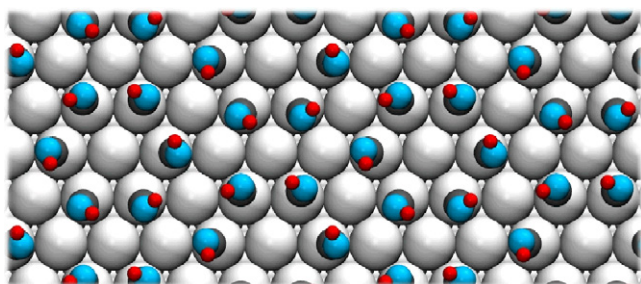
Fig. 11. Top view of a fully protonated $(2\sqrt{3} \times 2\sqrt{3})R30°$ cyanide-modified Pt(1 1 1) surfaces.

free Pt atoms was also examined in the presence of non-covalently attached K forming a *honeycomb* adlayer [17], and in the presence of a non-covalently attached K adlayer with the *center of the ring* structure. The results of these calculations are summarized in Table 7.

Interestingly, protonation of the N atoms of the adsorbed CNs of the $(2\sqrt{3} \times 2\sqrt{3})R30°$ structure is energetically very favorable, with an adsorption energy more than 1 eV larger than H bonded to the CN-free Pt atoms, which is barely affected by the presence of K and whose adsorption energy (Table 7) is roughly the same as on clean Pt(1 1 1) (Table 3). Formation of $(CN_{ad})_x$—H explains, hence, the experimentally observed 0.2 V positive shift of the onset of hydrogen adsorption. Our calculations also confirm that the effect of the alkaline cations on the CV of a cyanide modified Pt(1 1 1) electrode can be explained by a competition for the same adsorption sites, as we have suggested recently [17].

Finally, as illustrated in Fig. 11 and as suggested by the high value of the hydrogen adsorption energy of the Pt—CN—Hx1 structure (Fig. 10D and Table 2), the formation of $(CN_{ad})_x$—H is probably further stabilized by the formation of hydrogen-bonds between nitrogen atoms of neighboring cyanide groups in the hexagonal ring, as happens with the linear configuration (Fig. 8C and D).

Our theoretical calculations show that hydrogen adsorption *on top* of the free Pt atoms of the CN_{ad}-covered Pt(1 1 1) surface is also thermodynamically stable for all the configurations analyzed (Tables 4, 6 and 7). This supports the idea that, in the potential region between 0.6 V and 0.1 V, hydrogen adsorbs on the nitrogen atoms of the cyanide groups, but, at sufficiently negative potentials, and once all the available CN_{ad} sites have been occupied, hydrogen can also adsorb directly on the metal, and probably acts as the intermediate species in H_2 evolution.

4. Conclusions

DFT calculations cannot explain by themselves the preference for the experimentally observed structure adopted by cyanide on Pt(1 1 1) electrodes, suggesting that adsorption of cyanide forming a $(2\sqrt{3} \times 2\sqrt{3})R30°$ structure is driven by the presence of cations, other structures isoenergetic with it presenting cavities with sizes or geometries inappropriate for hosting the cations.

DFT calculations of the DOS projected onto those Pt atoms that are not directly bonded to CN show that the electronic structure of these atoms remains essentially unaltered, which demonstrates that CN_{ad} acts as an inert site blocker. For this reason, cyanide-modified Pt(1 1 1) electrodes are unique for studying atomic ensemble effects in electrocatalysis using the site-knockout strategy.

According to DFT calculations, protonation of the nitrogen atoms of CN_{ad} on Pt(1 1 1) is clearly favored over adsorption on a Pt atom. The positive shift in the onset of hydrogen adsorption in the CV of cyanide-modified Pt(1 1 1) electrodes can, hence, be qualitatively

explained by the formation of $(CN_{ad})_x$—H, instead of H bonded to the Pt atoms that remain free in the $(2\sqrt{3} \times 2\sqrt{3})R30°$ cyanide-modified Pt(1 1 1) structure. An analysis of the FTIR spectra shows that the Stark tuning rate of the CN stretching frequency of cyanide-modified Pt(1 1 1) changes at a potential coinciding with the onset of hydrogen adsorption in the corresponding CV, which can also be explained by the formation of $(CN_{ad})_x$—H.

Appendix A. Supplementary data

Supplementary data associated with this article can be found, in the online version, at doi:10.1016/j.electacta.2012.02.062.

References

[1] J.L. Stickney, S.D. Rosasco, G.N. Salaita, A.T. Hubbard, Langmuir 1 (1985) 66.
[2] V.B. Paulissen, C. Korzeniewski, J. Phys. Chem. 96 (1992) 4563.
[3] C.S. Kim, C. Korzeniewski, J. Phys. Chem. 97 (1993) 9784.
[4] C. Stuhlmann, Surf. Sci. 335 (1995) 221.
[5] Y.-G. Kim, S.-L. Yau, K. Itaya, J. Am. Chem. Soc. 118 (1996) 393.
[6] F. Huerta, E. Morallón, C. Quijada, J.L. Vázquez, A. Aldaz, Electrochim. Acta 44 (1998) 943.
[7] F.J. Huerta, E. Morallón, J. Vazquez, A. Aldaz, Surf. Sci. 396 (1998) 400.
[8] F. Huerta, E. Morallón, C. Quijada, J.L. Vázquez, L.E.A. Berlouis, J. Electroanal. Chem. 463 (1999) 109.
[9] F. Huerta, E. Morallón, J.L. Vázquez, Surf. Sci. 431 (1999) L577.
[10] F. Huerta, E. Morallón, J.L. Vázquez, Electrochem. Commun. 4 (2002) 251.
[11] I. Morales-Moreno, A. Cuesta, C. Gutiérrez, J. Electroanal. Chem. 560 (2003) 135.
[12] A. Cuesta, M. Escudero, Phys. Chem. Chem. Phys. 10 (2008) 3628.
[13] A. Cuesta, ChemPhysChem 12 (2011) 2375.
[14] D. Strmcnik, M. Escudero-Escribano, K. Kodama, V.R. Stamenkovic, A. Cuesta, N.M. Markovic, Nat. Chem. 2 (2010) 880.
[15] A. Cuesta, J. Am. Chem. Soc. 128 (2006) 13332.
[16] A. Cuesta, M. Escudero, B. Lanova, H. Baltruschat, Langmuir 25 (2009) 6500.
[17] M. Escudero-Escribano, M.E. Zoloff Michoff, E.P.M. Leiva, N.M. Marković, C. Gutiérrez, Á. Cuesta, ChemPhysChem 12 (2011) 2230.
[18] M. Escudero, J.F. Marco, A. Cuesta, J. Phys. Chem. C 113 (2009) 12340.
[19] M. Escudero-Escribano, PhD Thesis, Universidad Autónoma de Madrid, 2011, http://hdl.handle.net/10261/42378.
[20] B. Hammer, L.B. Hansen, J.K. Nørskov, Phys. Rev. B 59 (1999) 7413.
[21] J.M. Soler, E. Artacho, J.D. Gale, A. García, J. Junquera, P. Ordejón, D. Sánchez-Portal, J. Phys. Condens. Matter 14 (2002) 2745.
[22] W. Schmickler, Chem. Phys. Lett. 99 (1983) 135.
[23] M.I. Rojas, E.P.M. Leiva, J. Electroanal. Chem. 303 (1991) 55.
[24] M.I. Rojas, E.P.M. Leiva, Surf. Sci. 227 (1990) L121.
[25] K. Bange, T.E. Madey, J.K. Sass, E.M. Stuve, Surf. Sci. 183 (1987) 334.
[26] A. Cuesta, Surf. Sci. 572 (2004) 11.
[27] B.C. Schardt, J.L. Stickney, D.A. Stern, D.G. Frank, J.Y. Katekaru, S.D. Rosasco, G.N. Salaita, M.P. Soriaga, A.T. Hubbard, Inorg. Chem. 24 (1985) 1419.
[28] W. Daum, K.A. Friedrich, C. Klünker, D. Knabben, U. Stimming, H. Ibach, Appl. Phys. A 59 (1994) 553.
[29] K.A. Friedrich, W. Daum, C. Klünker, D. Knabben, U. Stimming, H. Ibach, Surf. Sci. 335 (1995) 315.
[30] F. Huerta, F. Montilla, E. Morallón, J.L. Vázquez, Surf. Sci. 600 (2006) 1221.
[31] A. Tadjeddine, A. Peremans, A. Le Rille, W.Q. Zheng, M. Tadjeddine, J.-P. Flament, J. Chem. Soc. Faraday Trans. 92 (1996) 3823.
[32] M. Tadjeddine, J.P. Flament, Chem. Phys. 240 (1999) 39.